

Effect of Load Cycling on the Consolidation Process For a Cohesive Soil

W. H. PERLOFF, JR., Assistant Professor of Civil Engineering, Ohio State University;

H. P. JOHNSON, Captain, U. S. Corps of Engineers, Fort Belvoir, Virginia; and

W. L. DE GROFF, Senior Laboratory Technician, Department of Civil Engineering, Ohio State University

One-dimensional consolidation tests, in which the load was cycled between fixed values, were performed on a sensitive Maine clay. Load cycling, up to 13 times, caused increased settlement with each cycle, but application of a pressure in excess of that applied during cycling caused a return to the original virgin curve. Both primary and secondary compression were reduced by load cycling. Pore water pressures measured at the base of single-drained specimens were of measurable magnitude during secondary compression.

•CONSOLIDATION of a saturated soil is the time-dependent decrease of soil volume due to the escape of water from the void in the soil mass. The classical analysis of one-dimensional consolidation (Terzaghi, 16) based on hydrodynamic principles, is the most commonly applied predictive method for handling consolidation problems. The consolidation experienced by a soil under a particular applied pressure increment is shown in Figure 1. The time-settlement curve in this figure is typical for one-dimensional consolidation tests on many cohesive soils. The dash line shows the time-settlement relation predicted by the classical consolidation theory. The portion of the consolidation predicted by the classical theory is commonly referred to as primary consolidation, and the additional portion is usually called secondary compression. Gray (4), Buisman (1), Taylor (15), Leonards and Girault (8) and Wahls (18) are among the many investigators who have examined secondary compression. Many hypotheses about its causes have been advanced although no generally accepted explanation has yet been proposed.

BACKGROUND

Effect of Secondary Compression on Time-Settlement Relation

The characteristic features of secondary compression and its influence on the time-settlement curve are shown in Figure 1. This curve is typical of results reported by many investigators. The theoretical and experimental curves usually agree quite well until approximately 60 to 70 percent of the theoretical consolidation has occurred. At that point the theoretical curve frequently falls below the experimental curve and then crosses the experimental curve again when almost 100 percent of the theoretical consolidation has occurred. For relatively large values of the time, the experimental curve becomes linear with the logarithm of time. Although exceptions to linearity have been reported (Hanrahan, 6; Palmer and Thompson, 13), Haefeli and Schaad (5) observed secondary compression to be linear with logarithm of time for load durations of about 3 yr.

The quantitative description of secondary compression is usually given by the amount of secondary compression occurring over one logarithmic cycle of time. When the

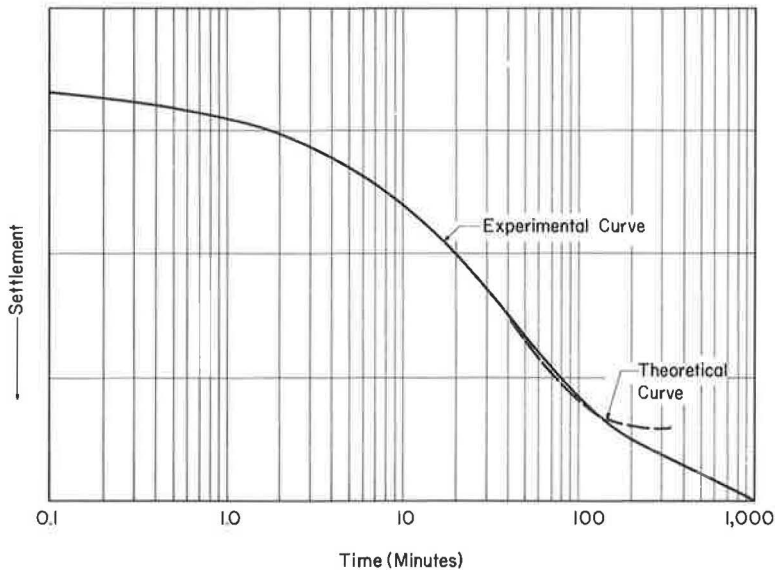


Figure 1. Typical time-settlement curve for one-dimensional consolidation test on cohesive soil.

consolidation curve is expressed in terms of void ratio change, the secondary compression is expressed by the coefficient of secondary compression, C_α , equal to the void ratio change occurring over one logarithmic cycle of time. When the consolidation curve is expressed in terms of settlement, secondary compression can be represented by the coefficient of secondary settlement, R_s , the settlement occurring over one logarithmic cycle of time. For one-dimensional compression, these two quantities are proportional, and will be used interchangeably hereafter.

Factors Affecting C_α (R_s)

Considerable research effort has been devoted to the study of the coefficient of secondary compression, and the factors affecting it. Moran et al. (10), Leonards and Girault (8), and Wahls (18) found that C_α varied with the total pressure applied to the soil specimen. A similar result was observed by Ray (14) for three-dimensional consolidation in a triaxial compression chamber. However, Taylor (15) and Newland and Allely (11) observed that C_α was independent of the total consolidation pressure. Girault (3), Newland and Allely (11), and Wahls (17) all agree that C_α is independent of the pressure increment ratio (the ratio of the applied pressure increment to the previous total pressure). Girault (3) inferred this from the fact that the ratio of secondary compression to primary consolidation, R_s/R_{100} (where R_{100} is the amount of settlement occurring during primary consolidation), depended on the pressure increment ratio in the same way as $1/R_{100}$.

It has been suggested in the past (Moran, et al., 10; Leonards and Ramiah, 9) that preloading reduces secondary compression. It was felt that if preloading once would reduce secondary compression, perhaps cycling of the load a sufficient number of times would completely eliminate it. To shed some additional light on the foregoing factors, a laboratory investigation was undertaken to examine the influence of load cycling on the consolidation process.

LABORATORY INVESTIGATION

Description of Soil

The soil tested was a sensitive gray, silty clay with black streaks from Clinton, Maine. Undisturbed samples of the soil were taken with $3\frac{1}{8}$ -in. diameter Shelby tubes

from a depth of 9 to 11 ft beneath the surface. The results of routine laboratory tests indicate the following properties:

| | |
|----------------------------|---------------------------------|
| Specific gravity of solids | 2.77 |
| Liquid limit | 33.0 percent |
| Plasticity index | 13.0 percent |
| Dry unit weight | 91.4 pcf |
| Field water content | 30.4 percent |
| Organic content | 0.7 by weight (ignition method) |
| Sensitivity | 7 |

The clay appears to have been deposited under marine conditions and subsequently uplifted, undergoing some leaching of salts from the pore fluid; it was normally consolidated and fully saturated.

Apparatus and Testing Procedures

All soil specimens were extruded from the 3 $\frac{1}{2}$ -in. diameter Shelby tubes and trimmed to fit snugly into consolidation rings. Fixed-ring consolidometers were used for all tests. The brass rings were liberally coated with Dow-Corning silicone grease to reduce the effects of side friction. All samples were 2 $\frac{1}{2}$ in. in diameter and 1 in. thick before consolidation.

Three specimens were consolidated with drainage permitted at both top and bottom of the specimens. These tests were carried out in a standard manner using dial gages with 0.0001-in. divisions to measure settlements. In addition, one specimen was consolidated in a specially modified fixed-ring consolidometer in which drainage was permitted only at the top, so that pore water pressure could be measured at the base of the specimen. The special consolidometer (Fig. 2) consists of a standard fixed-ring type of consolidometer with the bottom porous stone replaced by a brass plug with a smaller porous stone inserted in it. Two outlets are provided for the water at the base leading into temperature-compensated electrical pressure transducers, a Dynisco PT 25 with a range of pressure from 0 to 100 psi, and a Dynisco PT 85 with a range from 0 to 1 psi. This special low pressure transducer was isolated from the system by a valve to protect it from overloading. Excitation of the pressure transducers was accomplished with B and F model 110-T input conditioners with zener diode regulated voltage outputs. In addition, a thermistor (temperature sensitive resistance) was mounted inside the consolidometer underneath the specimen to permit observation of temperature.

Settlement of the specimen was measured by Daytronic 103C-200 linear variable differential transformer (LVDT). Outputs from the pressure transducers and the LVDT were fed into Varian G-14 strip-chart recorders, and recorded continuously as a function of time. It was possible to record accurately pressure changes as small as that created by $\frac{1}{4}$ mm of water when using the PT 85. Settlements of 5×10^{-6} in. could also be observed. Temperature changes were recorded on a Bausch and Lomb V. O. M. 5 strip-chart recorder and could be observed with an accuracy of 0.05 C.

Accuracy of the recorded variables was continually checked. The zero setting of the pressure transducers was checked daily. Correct calibration of the pressure transducers was verified every second or third day. The LVDT and thermistor circuits were calibrated before the test started and checked at the end of the test. No variations were observed in the response of the various transducers of sufficient magnitude to influence the results.

Description of Tests

The cyclic loading was accomplished by applying pressure increments to the soil to some predetermined pressure on the virgin curve. The soil was rebounded in the standard manner to a predetermined pressure, with each rebound increment remaining at least 24 hr. Pressure increments were then reapplied, in the same manner as for the initial loading until the previous maximum pressure was reached. In this way, one cycle was completed. The process was repeated for all additional cycles.

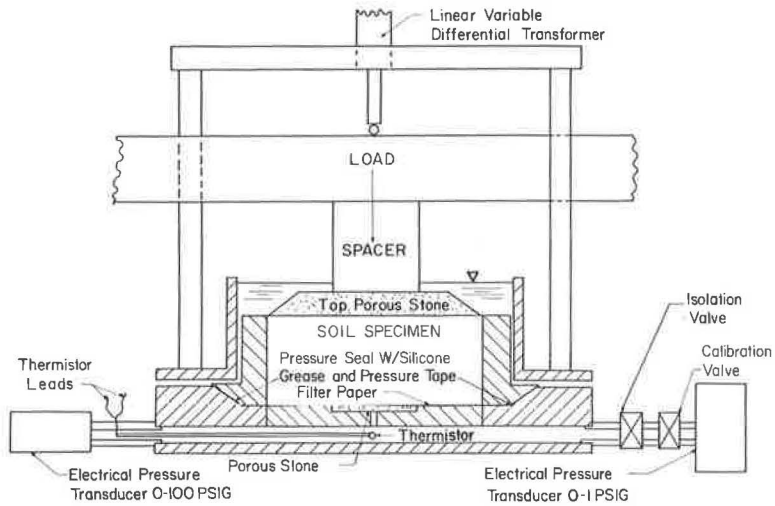


Figure 2. Single-drained consolidometer with provisions for pore water pressure and temperature measurement.

TABLE 1
SUMMARY OF TESTS

| Specimen No. | Max. Press. Before Cycling (kg/cm ²) | Cyclic Loading | | No. of Recomp. Cycles | Duration of Test (days) |
|----------------|--|--|---|-----------------------|-------------------------|
| | | Min. Press. (rebound to) (kg/cm ²) | Max. Press. (reload to) (kg/cm ²) | | |
| 1 ^a | 11.50 | 1.44 | 11.50 | 13 | 215 |
| 2 ^a | 22.99 | 2.87 | 22.99 | 13 | 211 |
| 3 ^a | 5.75 | 0.719 | 5.75 | 13 | 213 |
| 4 ^b | 7.54 | 0.228 | 7.54 | 3 | 80 |

^aDouble drained.

^bSingle drained.

A pressure increment ratio of approximately 1 was used for all tests. On all initial loadings and for the first few reloadings, the pressure increment duration was 48 hr. During later load cycles, when the time to 100 percent consolidation was very short, the time was reduced to 24 hr. Each of the specimens was cycled over a different range of pressure to obtain an indication of the influence of the magnitude of pressure on the results.

Table 1 gives a summary of the tests reported. At the end of 13 recompression cycles, specimens 1 and 3 were loaded to a total pressure of 22.99 kg/sq cm before the final rebound. Specimen 4 was loaded to 15.05 kg/sq cm after 3 recompression cycles.

TEST RESULTS

Settlement-Pressure Relationships

The relationship between settlement and pressure after 24 hr under a given load increment is shown in Figures 3 through 5 for specimens 1-3. (Figure 3c also shows the effect of load cycling on time-settlement curves for double-drained specimen 1.) The curve in Figure 6, for specimen 4, is for settlements at the Casagrande 100 percent consolidation point. Results of the cyclic loading are shown in detail in Figures 3b,

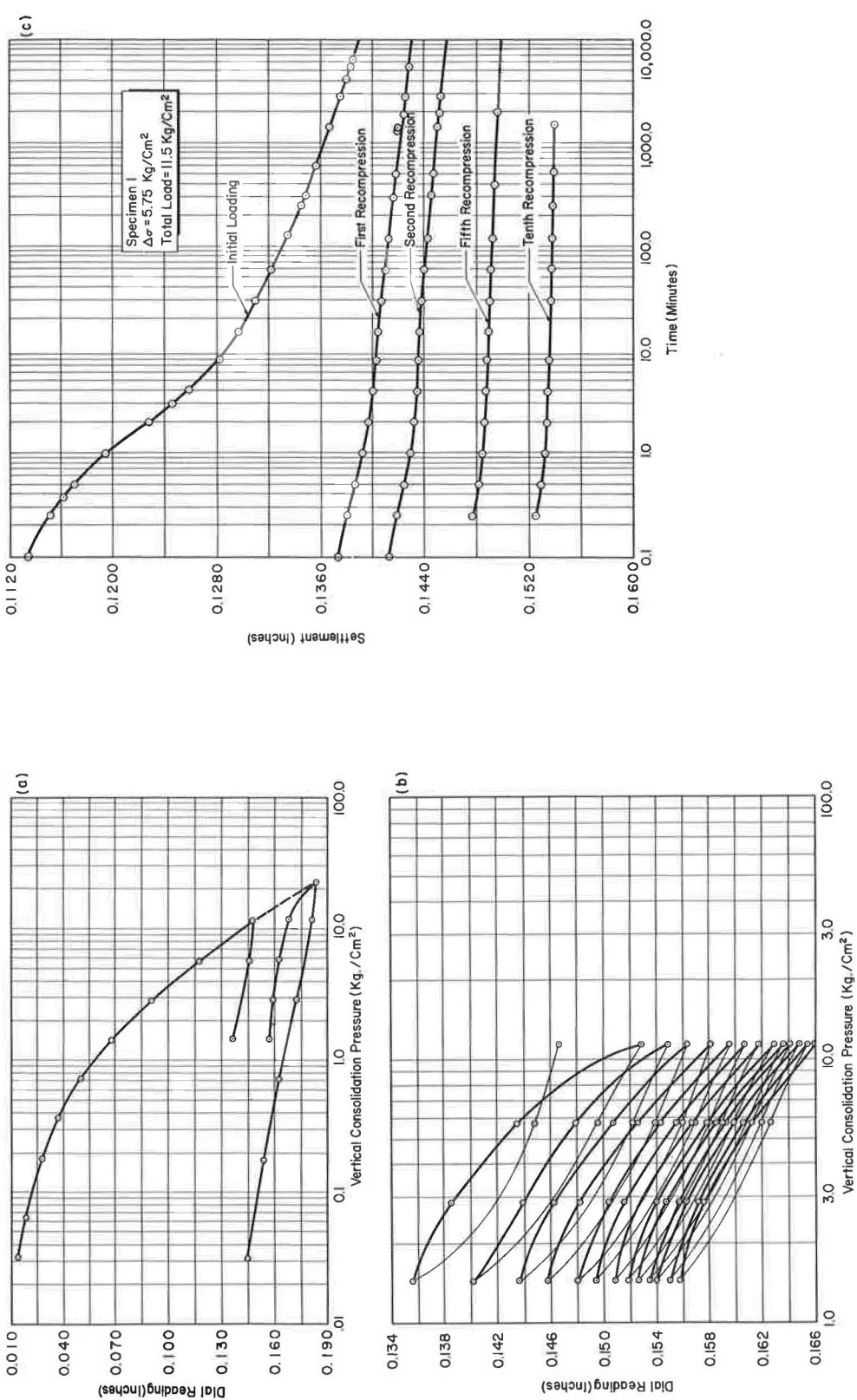


Figure 3. Relationship between consolidation pressure and settlement for specimen 1: (a) initial and final loading; (b) load cycling; (c) effect of load cycling on the time-settlement curves for a double drained specimen.

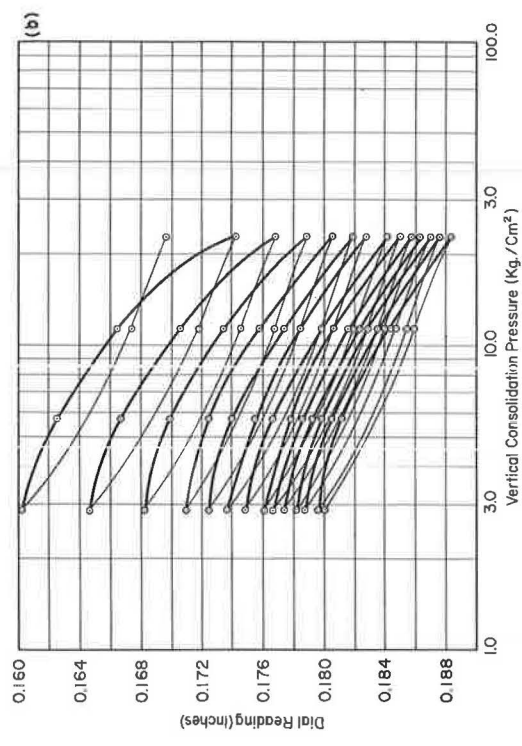
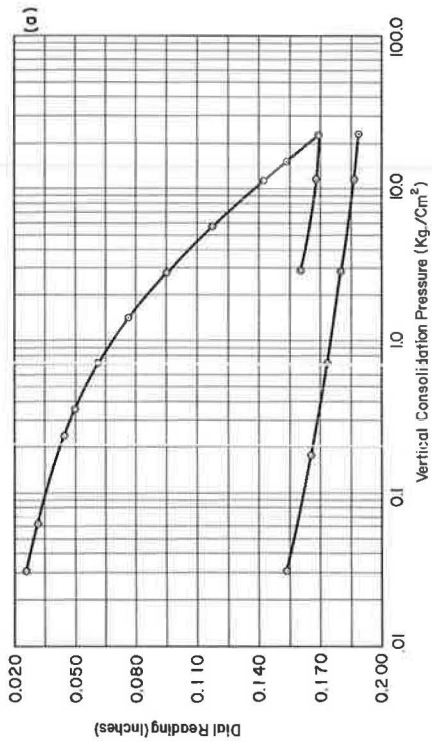


Figure 4. Relationship between consolidation pressure and settlement for specimen 2: (a) initial and final loading, and (b) load cycling.

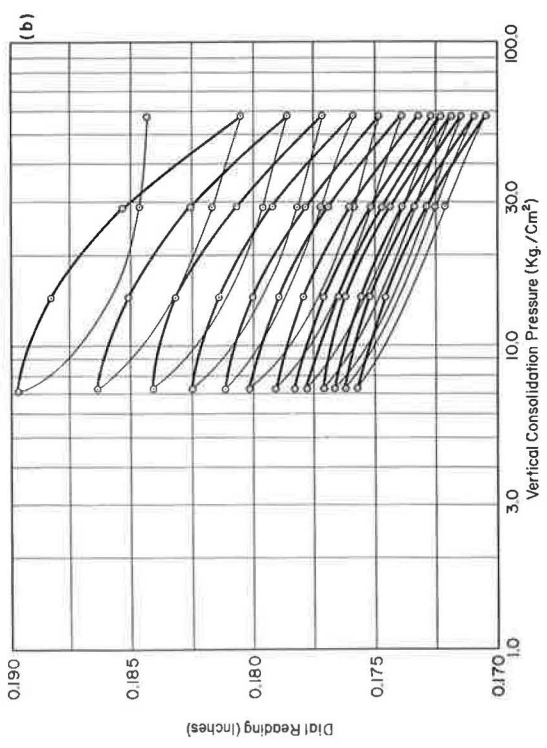
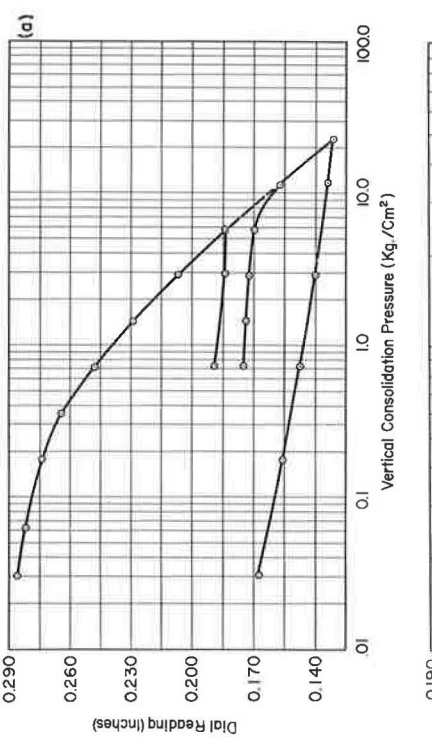


Figure 5. Relationship between consolidation pressure and settlement for specimen 3: (a) initial and final loading, and (b) load cycling.

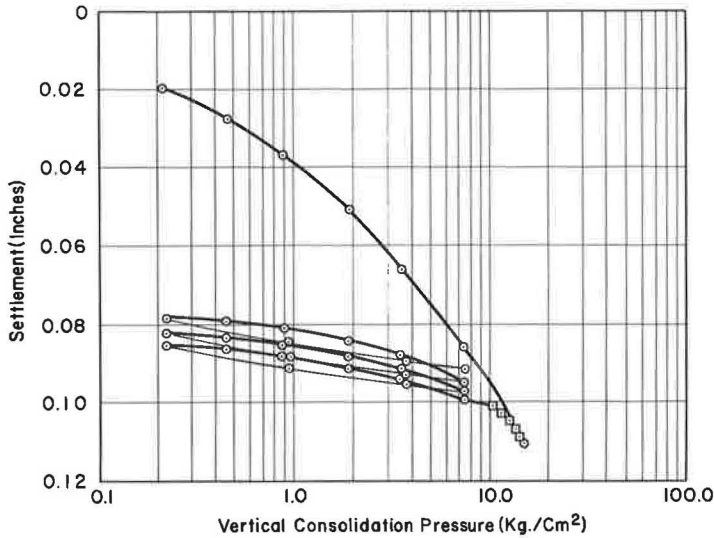


Figure 6. Relationship between consolidation pressure and settlement for specimen 4.

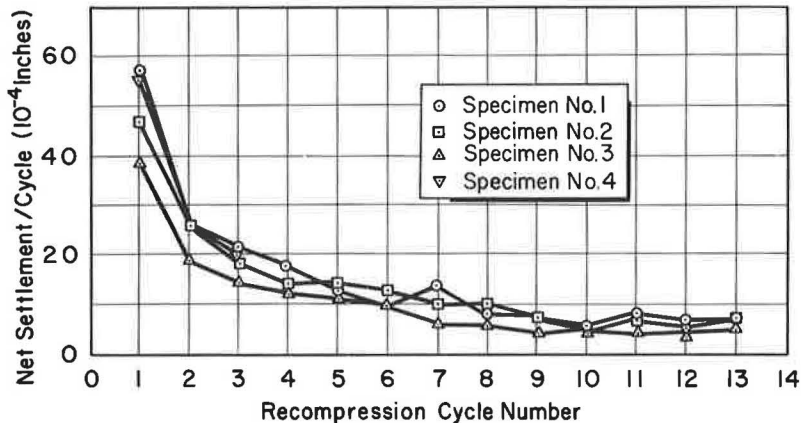


Figure 7. Effect of number of recompression cycles on net settlement.

4b, 5b, and 6 for the four specimens, where the reloading curves are shown as heavy lines and the rebound curves as lighter lines to facilitate interpretation. The net displacement for each hysteresis loop decreases as the number of cycles increases. In addition, there is a decrease in the size of the hysteresis loops for each successive cycle of loading.

The net reduction in sample thickness for each load cycle is shown as a function of the number of recompression cycles in Figure 7. The results do not definitely indicate whether the net settlement will approach zero after some large number of cycles. Tentative extrapolation of the results suggests that at least 50 cycles would be required to reduce the net settlement to zero.

At the end of 13 load cycles for specimens 1 through 3, and three load cycles for specimen 4, the specimens were loaded to the next higher pressure. Figures 3a, 5a, and 6 show that the settlement-pressure relationship returns to the virgin compression

curve. Since continuous pore water pressure measurements were made at the base of specimen 4, it was possible to estimate the average effective consolidation pressure at each point during the increment. This was done using the expressions presented by Perloff et al. (12) for the pore water pressure distribution throughout a consolidating specimen which include the influence of flexibility of the pressure measuring system on this distribution. The method by which these equations have been used to determine the average effective consolidation pressure is given in the Appendix. With the average effective consolidation pressure known, the shape of the settlement-pressure curve between the end points can be determined for the last applied pressure increment, and is shown in Figure 6 as the portion of the curve indicated by the small rectangles. It appears that load cycling has a prestressing effect on the soil, since the preconsolidation pressure determined from this curve is distinctly higher than the previously applied maximum pressure. This is not surprising since the void ratio is less than that on the virgin curve under the initial loading. This effect appears similar to the "quasi-preconsolidation pressure" reported by Leonards and Ramiah (9) and Leonards and Altschaeffl (7) for consolidation tests in which a given pressure has remained on a specimen much longer than the ordinary time increment.

Coefficient of Secondary Settlement (R_s)

The coefficients of secondary settlement, R_s , are shown in Figure 8 as a function of the effective consolidation pressure for the initial loading for the four specimens. The magnitude of R_s increases as the effective consolidation pressure increases to a pressure of approximately three times the preconsolidation pressure, at which point the magnitude of R_s remains more or less constant. This result is consistent with data presented by Leonards and Girault (8) and Wahls (18) for one-dimensional consolidation tests, and data presented by Ray (14) for triaxial consolidation tests.

These data imply that the magnitude of R_s is independent of the length of the drainage path for a given specimen thickness because the values of R_s are the same for specimen 4 as for the other three specimens, even though specimen 4 was single-drained and the others were double-drained.

The influence of load cycling on the magnitude of R_s is shown in Figure 9, where the ratio of R_s at the end of the n th load cycle, R_{sn} , to R_s for the initial loading at that pressure, R_{sj} , is a function of number of recompression cycles. The magnitude of R_s is reduced to about 36 to 38 percent of its initial value in the first recompression cycle. As the number of recompression cycles increases, R_s decreases to approximately 5 to 8 percent of its initial value, at which point it remains essentially constant with continued load cycling, at least for the number of cycles observed in the study. The curves appear quite similar even though each curve corresponds to a different magnitude of load. Furthermore, there does not seem to be any effect of length of drainage path, for a given specimen thickness, on the ratio R_{sn}/R_{sj} .

The effect of load cycling on the ratio of the coefficient of secondary settlement, R_s , to the amount of settlement occurring during primary consolidation, R_{100} , was introduced by Girault (3) as an indicator of the shape of the time-settlement curve. A small value of R_s/R_{100} indicates a curve which approximates the theoretical curve. A large value of R_s/R_{100} indicates substantial deviation from the Terzaghi curve, particularly at times near and after the 100 percent point. Girault found that R_s/R_{100} was a function of the pressure-increment ratio. He reported results of tests on Mexico City and Bedford clays and showed that R_s/R_{100} varied from 0.8 to 1.0 at a pressure-increment ratio of approximately 0.15. The ratio R_s/R_{100} decreased rapidly as the pressure-increment ratio increased, with values as small as 0.05 to 0.1 at a pressure-increment ratio of 3. At a pressure-increment ratio of one, Girault (3) found that R_s/R_{100} varied from approximately 0.05 to 0.15. Table 2 gives the magnitude of R_s/R_{100} at each pressure for the initial and recompression cycles for specimen 4, tested at a pressure-increment ratio of approximately 1. Due to the hydraulic loading arrangement used for testing this specimen, the actual pressure-increment ratio varied from 0.87 to 1.12. Almost all of the values of R_s/R_{100} lie between 0.1 and 0.2, indicating that the shape of the time settlement curve is essentially the same after cycling of the load as before.

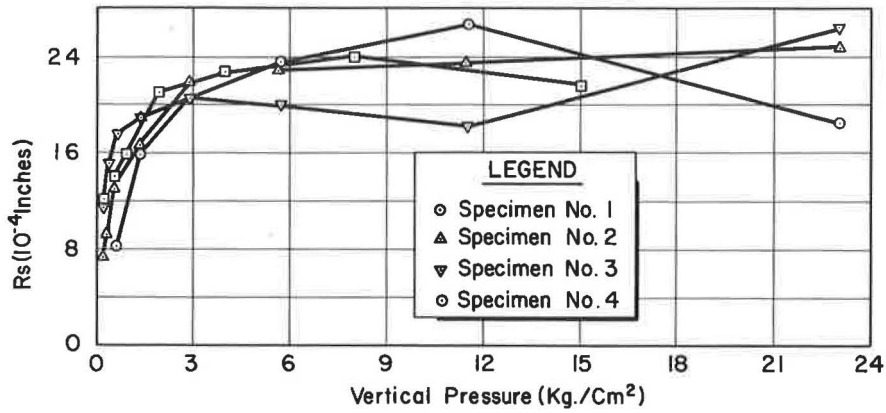


Figure 8. Effect of consolidation pressure on coefficient of secondary settlement (R_s).

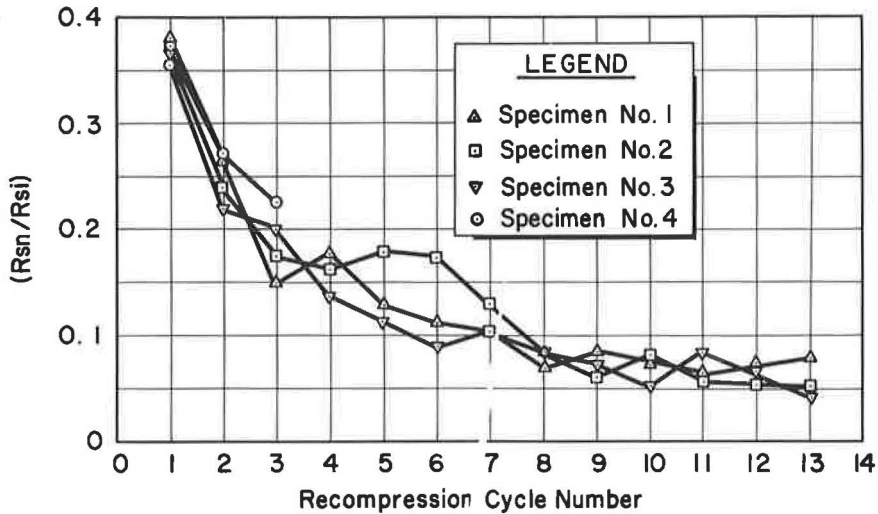


Figure 9. Effect of number of recompression cycles on the coefficient of secondary settlement.

TABLE 2
EFFECT OF LOAD CYCLING ON R_s/R_{100} FOR SPECIMEN 4

| Pressure (kg/cm ²) | Initial Increment | Cycle 1 | Cycle 2 | Cycle 3 |
|--------------------------------|-------------------|---------|---------|---------|
| 0.216 | 0.071 | | | |
| 0.465 | 0.062 | 0.114 | 0.110 | 0.133 |
| 0.903 | 0.230 | 0.112 | 0.090 | 0.114 |
| 1.918 | 0.185 | 0.099 | 0.081 | 0.094 |
| 3.580 | 0.206 | 0.114 | 0.100 | 0.095 |
| 7.540 | 0.160 | 0.186 | 0.157 | 0.151 |
| 15.050 | 0.191 | | | |

It appears that whatever prestress effects are induced by cycling of the load, the secondary compression is affected in essentially the same way as the magnitude of primary consolidation.

Pore Water Pressure Dissipation as a Function of Time

The classical consolidation theory is formulated in terms of pore water pressure dissipation. Void ratio changes are inferred from the assumption that volume changes of the soil mass are proportional to the pressure dissipation. According to the classical theory, pore water pressure dissipates to zero at the end of primary consolidation. Many investigators have attempted to determine if, in fact, this is the case. Hanrahan (6) and Girault (3) presented data indicating that the pore water pressure approaches zero shortly after primary consolidation has ceased. Crawford (2) showed results suggesting that pore water pressure at the base dissipated to zero after about 1 day for specimens which reached 100 percent consolidation (as determined by the Casa-grande construction) in 100 to 200 min.

Curves of pore water pressure dissipation as a function of time are shown in Figures 10-13 for a typical initial pressure increment and the three corresponding recompression increments, along with the time-settlement curves. The theoretical pore water pressure dissipation curves were determined using the expression presented by Perloff et al. (12) to account for the effect of system flexibility on pore water pressure measurement at the base of one-dimensional consolidation specimens. System flexibility is especially important when the soil has been highly precompressed by cyclic loading because the stiffness of the measuring system relative to that of the soil structure is substantially reduced. The reason for the extremely low peak pore water pressure in Figure 10 is that the hydraulic loading arrangement used in these tests experienced some lag in following the specimen deformation for the initial increment when deformations were relatively large. This did not seem to be as much of a problem in the recompression increments as indicated by the relative agreement between the peak magnitude measured and theoretical pore water pressures shown in Figures 11 through 13.

The pore water pressure at the base of the specimen does not decrease to zero, for the time duration shown in Figures 10-13, even though the theoretical 100 percent consolidation points for the recompression increments occur at approximately 10 min. Increments have been carried out for as long as 72 hr without observation of zero pore water pressure. However, at very long periods of time, when the excess pore water pressure has dissipated to less than 2 cm of water, small variations in temperature cause variations in the magnitude of pressure greater than the magnitude of the pressure itself. Figure 14 shows the variations in temperature at the base of the specimen, pore water pressure at the base, and settlement over a 4-hr period starting approximately 35 hr after the application of the pressure increment. A moderately rapid reduction in temperature causes a corresponding reduction in pore water pressure and a slackening of the settlement curve. With moderately rapid temperature fluctuations (Fig. 14), the pressure may even become negative for very small values of pressure until the temperature decrease occurs at a reduced rate, ceases, or becomes a temperature increase. Although the general trends of the time-settlement and time-pore water pressure curves are unchanged, it is obvious that at very small pressures, small temperature variations tend to mask the results. It seems likely that these changes occurring over short time spans are probably due to expansion and contraction of the water in the specimen and in the cavity underneath the porous stone. It appears here that not only the temperature but the rate of temperature change is particularly significant. This can be seen by observing the close correspondence of the breaks in the pressure and settlement curves with changes in rate of temperature change. Present tests are being conducted in a specially prepared constant temperature chamber which will insure constant specimen temperature within ± 0.05 C.

In spite of the influence of temperature changes at very small pressures, the data indicate that the pore water pressure at the base does not dissipate to zero, at least over the time span measured.

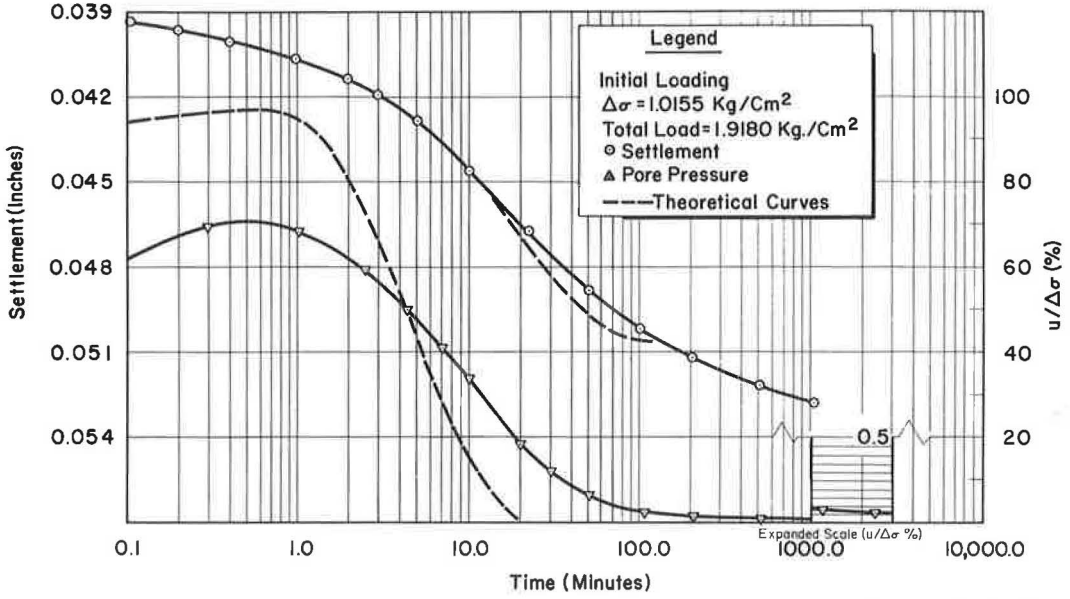


Figure 10. Consolidation behavior of single-drained specimen (specimen 4) for typical pressure increment.

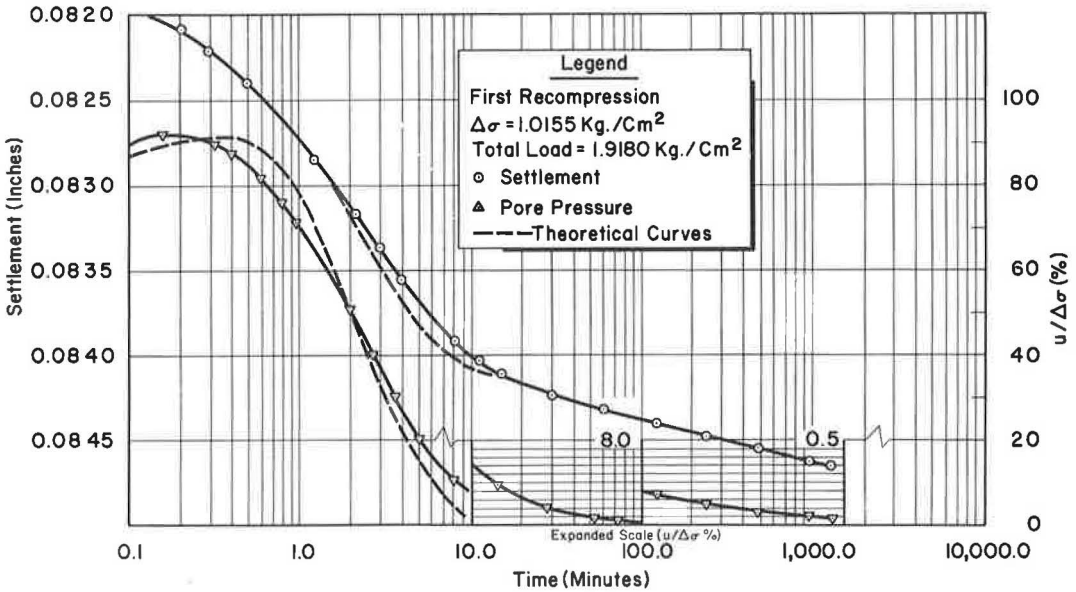


Figure 11. Consolidation behavior of single-drained specimen (specimen 4) for typical pressure increment.

CONCLUSIONS

Based on the foregoing results, the following conclusions can be drawn, at least for one-dimensional consolidation tests on a sensitive undisturbed clay:

1. Pore water pressures exist and are of measurable magnitude during secondary compression. The pressure at the base did not go to zero for as long as the tests were conducted.

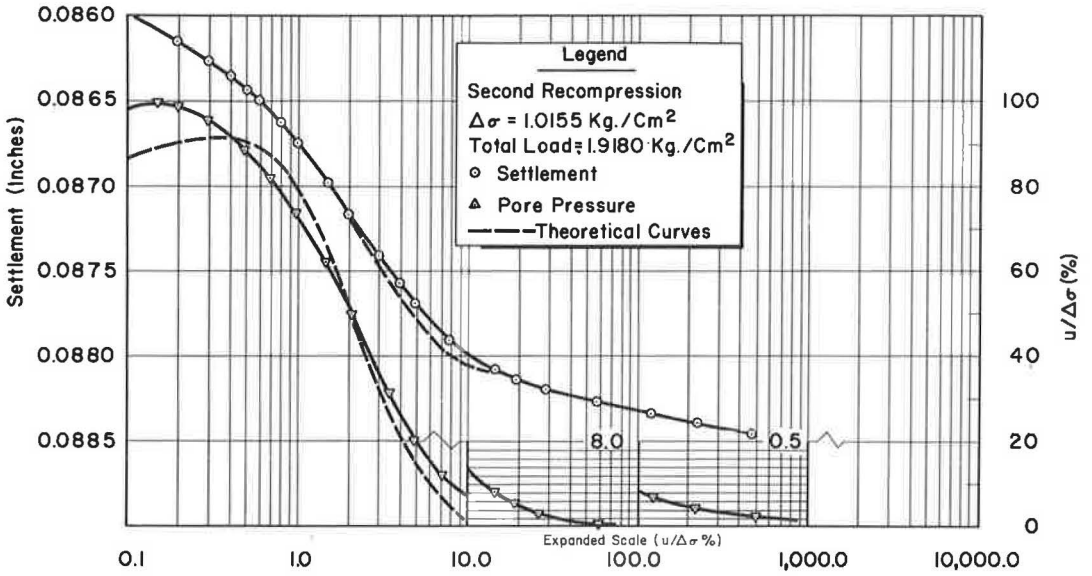


Figure 12. Consolidation behavior of single-drained specimen (specimen 4) for typical pressure increment.

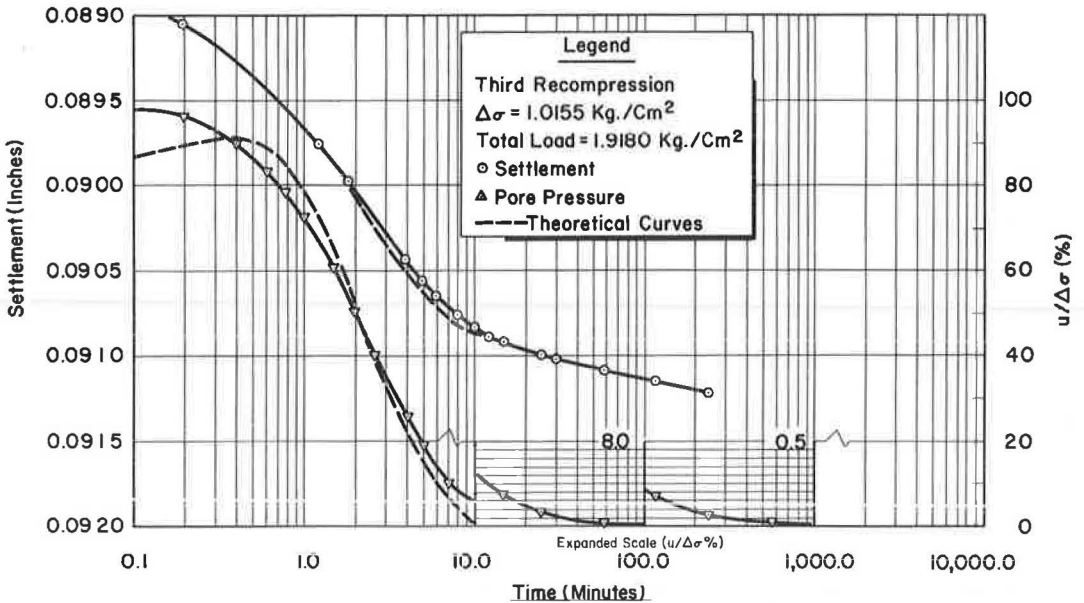


Figure 13. Consolidation behavior of single-drained specimen (specimen 4) for typical pressure increment.

2. Cyclic loading produces a net settlement for each cycle. However, the net settlement decreases as the number of cycles increases and approaches a very small value. The data available do not indicate whether a zero net settlement will result from a sufficiently large number of load cycles.

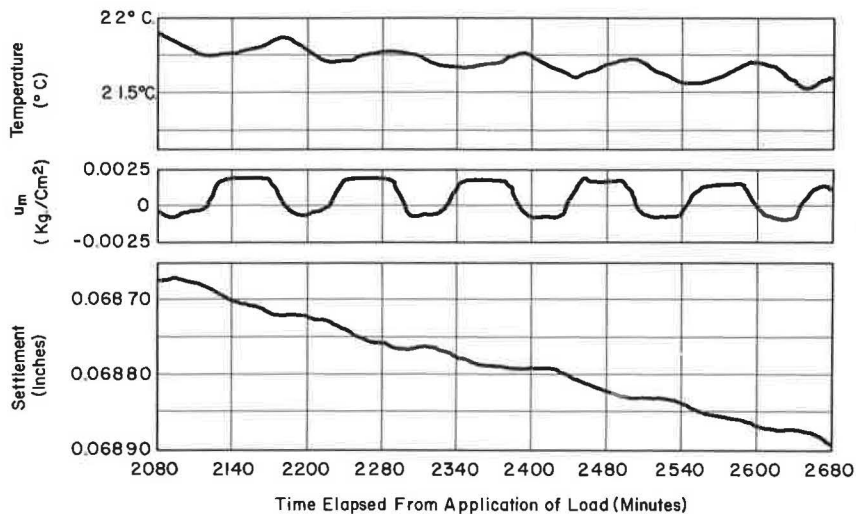


Figure 14. Effect of temperature on pore water pressure at base and settlement during secondary compression.

3. Load cycling reduces the amounts of primary and secondary compression to a small fraction of their initial magnitudes under a given load. However, the cycling does not appear to affect the shape of the time-settlement curve, as expressed by the ratio R_s/R_{100} .

4. The settlement-pressure curve returns to the original virgin curve after load cycling. The load cycling appears to induce a prestress effect since the return to the virgin curve is characterized by the presence of a "quasi-preconsolidation pressure" larger than the actual preconsolidation pressure.

5. The limited data available indicate that the coefficient of secondary settlement, R_s , is independent of the length of drainage path for a given specimen thickness.

6. The flexibility of the pore pressure measuring system becomes significant when the soil is subjected to load cycling, due to the low value of compressibility for the highly precompressed soil. Use of the theoretical expression from Perloff et al. (12) assists in accounting for this effect.

7. Temperature effects are important, even for small temperature variations, when very low pore water pressures are measured during secondary compression.

REFERENCES

1. Buisman, A. S. Results of Long Duration Settlement Tests. Proc. First International Conference on Soil Mechanics and Foundation Eng., Cambridge, Vol. I, p. 103, 1936.
2. Crawford, C. B. Interpretation of the Consolidation Test. Jour. of Soil Mechanics and Foundation Div., ASCE, Vol. 90, No. SM5, Sept. 1964.
3. Girault, P. A Study on the Consolidation of Mexico City Clay. Ph. D. thesis, Purdue Univ., Lafayette, Indiana, 1960.
4. Gray, Hamilton. Progress Report on Research on the Consolidation of Fine-Grained Soils. Proc., First Internat. Conf. on Soil Mechanics and Foundation Eng., Vol. 2, Cambridge, p. 138, 1936.
5. Haefeli, R. and Schaad, W. Time Effects in Connection with Consolidation Tests. Proc. Sec. Intern. Conf. on Soil Mechanics and Foundation Eng., Vol. III, Rotterdam, p. 23, 1948.
6. Hanrahan, E. T. An Investigation of Some Physical Properties of Peat. Geotechnique, Vol. 4, No. 3, p. 108, Sept. 1954.

7. Leonards, G. A. and Altschaeffl, G. A. The Compressibility of Clay. Jour. of Soil Mechanics and Foundation Div., ASCE, Vol. 90, No. SM5, Sept. 1964.
8. Leonards, G. A. and Girault, P. A Study of the One-Dimensional Consolidation Test. Proc., Fifth Internat. Conf. on Soil Mechanics and Foundation Eng., Paris, Vol. I, p. 213, 1961.
9. Leonards, G. A. and Ramiah, B. K. Time Effects in the Consolidation of Clay. Symp. on Time-Rate of Loading in Testing Soils, Spec. Tech. Publ. No. 254, ASTM, 1960.
10. Moran, Proctor, Mueser, and Rutledge. Study of Deep Soil Stabilization by Vertical Sand Drains. Rept. II, Bur. of Yards and Docks, Dept. of Navy, June 1958.
11. Newland, P. L. and Allely, B. H. A Study of the Consolidation Characteristics of a Clay. Geotechnique, Vol. 10, No. 2, p. 62, June 1960.
12. Perloff, W. H., Nair, K., and Smith, J. G. Effect of Measuring System on Pore Water Pressure in the Consolidation Test. Proc., Sixth Internat. Conf. on Soil Mechanics and Foundation Eng., in press, 1965.
13. Palmer, L. and Thompson, J. Report of Consolidation Tests with Peat. Symp. on Consolidation Testing of Soils, Spec. Tech. Publ. No. 126, ASTM, p. 4, June 1951.
14. Ray, J. W. The Effect of the Principal Stress Ratio on Secondary Compression in Cohesive Soils. M. S. thesis, Ohio State Univ., Columbus, Ohio, March 1963.
15. Taylor, D. W. Research on Consolidation of Clays, Dept. of Civil and Sanitary Eng., MIT, Ser. 32, Aug. 1942.
16. Terzaghi, K. Die Berechnung der Durchlässigkeitsziffer des Tones aus dem Verlauf der hydrodynamischen Spannungserscheinungen. Akademie der Wissenschaften in Wien. Sitzungsberichte. Mathematisch-naturwissenschaftliche Klasse. Pt. IIa, Vol. 132, No. 3-4, pp. 125-138.
17. Wahls, H. E. Primary and Secondary Effects in the Consolidation of Cohesive Soils. Ph. D. thesis, Northwestern Univ., Evanston, Ill., 1961.
18. Wahls, H. E. Analysis of Primary and Secondary Consolidation. Jour. of Soil Mechanics and Foundation Div., ASCE, Vol. 88, No. SM6, Dec. 1962.

Appendix

METHOD FOR DETERMINING AVERAGE EFFECTIVE CONSOLIDATION PRESSURE

To determine the shape of the settlement-pressure curve for a given pressure increment, it is necessary to know the average effective consolidation pressure at a given time, $(\sigma'_c)_t$, defined as

$$(\sigma'_c)_t = \sigma_c - (u_{avg})_t \quad (1)$$

where σ_c is the applied vertical consolidation pressure, and $(u_{avg})_t$ is defined by

$$(u_{avg})_t = \frac{1}{H} \int_0^H u(x, t)_t dx \quad (2)$$

where x is the depth from the top of a one-dimensional consolidation specimen, H is the thickness, $u(x, t)_t$ is the pore water pressure isochrone corresponding to time t .

The expression for $u(x, t)$ for a one-dimensional consolidation test in which pore water pressures are measured at the base of the specimen, with a flexible system is given by Perloff et al. (12) as

$$u(x, t) = 2u_0 \sum_{n=1}^{\infty} \frac{(A_n + \eta^2/A_n) \sin A_n - \eta}{(A_n^2 + \eta^2 + \eta) \sin A_n} \sin \frac{A_n x}{H} e^{-A_n^2 T} \quad (3)$$

where

u_0 = initial uniform pore water pressure for $0 < x < H$ (equal to applied pressure increment, $\Delta\sigma$);

$\eta = \frac{AHm_v}{\lambda}$ = stiffness of measuring system relative to that of soil skeleton;

A = specimen area;

H = specimen thickness;

m_v = the coefficient of volume compressibility of the soil;

λ = volumetric compliance of pore water pressure measuring system, i.e., the system volume demand per unit pressure change;

A_n = positive roots of the $A_n \tan A_n = \eta$;

e = base of natural logarithms; and

$T = \frac{c t}{H^2}$ = a dimensionless time factor.

Eq. 3 was derived on the basis of the classical hydrodynamic consolidation assumptions about soil properties.

Substituting Eq. 3 into Eq. 2 and integrating gives the theoretical expression for u_{avg} :

$$u_{avg} = 2u_0 \sum_{n=1}^{\infty} \frac{(A_n + \eta^2/A_n) \sin A_n - \eta}{A_n (A_n^2 + \eta^2 + \eta) \sin A_n} (1 - \cos A_n) e^{-A_n^2 T} \quad (4)$$

When $\eta = \infty$, Eq. 4 reduces to the Terzaghi (16) equation for a single drained specimen.

The theoretical value of the measured pore water pressure at the base (Perloff et al., 12) is

$$u_{meas} = 2u_0 \sum_{n=1}^{\infty} \frac{(A_n + \eta^2/A_n) \sin A_n - \eta}{A_n^2 + \eta^2 + \eta} e^{-A_n^2 T} \quad (5)$$

Solving Eq. 5 for u_0 and substituting this into Eq. 4 gives the average pore water pressure in terms of the measured pore water pressure at the base:

$$u_{avg} = u_{meas} \frac{\sum_{n=1}^{\infty} \frac{(A_n + \eta^2/A_n) \sin A_n - \eta}{A_n (A_n^2 + \eta^2 + \eta) \sin A_n} (1 - \cos A_n) e^{-A_n^2 T}}{\sum_{n=1}^{\infty} \frac{(A_n + \eta^2/A_n) \sin A_n - \eta}{A_n^2 + \eta^2 + \eta} e^{-A_n^2 T}} \quad (6)$$

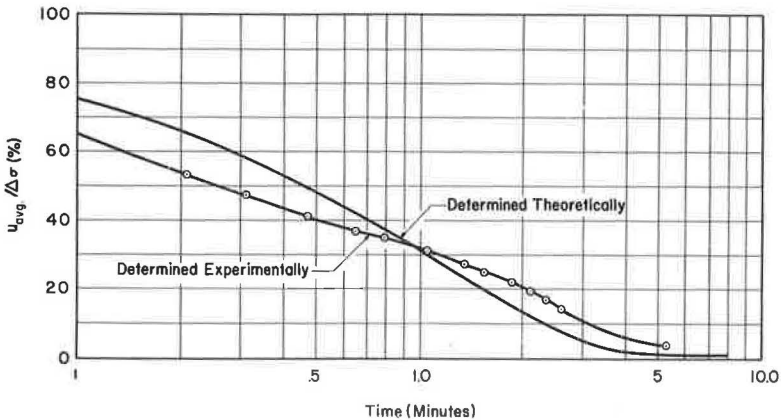


Figure 15. Comparison of average pore water pressure determined theoretically and experimentally.

Thus, if the measured pore water pressure at the base of the specimen is known, the average pore water pressure, and therefore the effective consolidation pressure, can be determined.

If the measured value of u_{meas} were identical to that predicted by Eq. 5, then Eqs. 4 and 6 would lead to identical results. In such a case, it would not be necessary to measure pore water pressures to know σ_b^i . However, when the measured and theoretical pore water pressures at the base are not equal, Eqs. 4 and 6 lead to very different results. This is illustrated in Figure 15, which shows the relationship between u_{avg} and time, as predicted by Eq. 4, and as predicted by Eq. 5 using the measured pore water pressure, for the last pressure increment applied to specimen 4 (Fig. 6). The relationship determined from the measured pressures is not the same as that from purely theoretical considerations.

The validity of Eq. 6 depends on the assumption that the relationship between u_{avg} and u_{meas} will be the same at a given time factor, even if the magnitude of u_{meas} is different from that predicted by theory. This assumption is probably reasonable, at least for time factors greater than 0.1 ($t = 0.26$ min for this increment), because the ratio of the two series in Eq. 6 changes very little as the time factor changes, when $T > 0.1$.